Transportation Geotechnics 39 (2023) 100933

Contents lists available at ScienceDirect

Transportation Geotechnics

journal homepage: www.elsevier.com/locate/trgeo

Effect of spatial variability of soil properties and geostatistical conditional simulation on reliability characteristics and critical slip surfaces of soil slopes

A.R. Kalantari [a], A. Johari [a,*], M. Zandpour [a], M. Kalantari [b]

[a] Dept. of Geotechnical and Civil Engineering, Shiraz Univ. of Technology, Shiraz 71557-13876, Iran
[b] School of Engineering, Department of Civil and Environmental Engineering, Shiraz University, Shiraz, Iran

ARTICLE INFO

Keywords:
Critical slip surface
Geostatistical conditional simulation
Random finite element method
Slope stability
Soil heterogeneity

ABSTRACT

Evaluation of the stability and determination of the Critical Slip Surface (CSS) of soil slopes are salient topics in geotechnical engineering. On the other hand, the stability and CSS are not only affected by soil heterogeneity but also by the boreholes' location and method of predicting soil parameters in the domain of analysis. The unconditional simulation in which known data and its location are not incorporated may lead to results far from reality. Moreover, in some conditional simulations, the borehole data are directly mapped into the analysis section without taking the location of the known data into account, which can either overestimate or underestimate the stability of the slope. In the current study, the Finite Element Method (FEM) is coupled with the geostatistical method to evaluate the reliability characteristics and CSS distribution with consideration of the known data, location of boreholes, uncertainty of surcharge load, and soil heterogeneity. The results of a real case demonstrate that in comparison to the unconditional simulation, utilizing the conditional simulation improves the distribution of Factor of Safety (FS) by up to 14% while decreasing the related standard deviation by 4% to 40%. Moreover, conditional simulation offers a significant reduction in uncertainty of the slip surface and unsafe distance from the edge of the slope. Besides, it is concluded that soil heterogeneity has a major impact on CSS distribution and induces the local CSS, which cannot occur on a homogeneous slope.

Introduction

The instability of soil slopes can cause great amounts of damage and loss of life. Hence, it is vital to assess the stability of the slopes and associated risks. The analysis of slope stability involves estimating the safety index and determining the location of the CSS. To assess the performance of the soil slopes, considering not only the uncertainty of soil properties and applied loads but also the known data and its location are essential. There are several different methods available for slope stability analysis. The most commonly adopted ones are the Limit Equilibrium Method (LEM), Limit Analysis Method, and FEM.

Although the traditional deterministic stability analysis is widely used in engineering practice, it cannot explicitly account for the various geotechnical-related uncertainties and provide no information on the variability of the safety margin. In the early'70s, a reliability-based method is proposed as a complementary measure to the FS to aid engineers in making acceptable designs. Then due to the disability of the probabilistic method to take the soil heterogeneity into account, in the early'90s, Griffiths and Fenton [1] proposed a new probabilistic analysis approach, namely the Random Finite Element Method (RFEM). After that, several kinds of research have been conducted to assess the reliability characteristics and the location of CSS in soil slopes [2,3]. For instance, Griffiths et al. [4] investigated the probability of slope failure using both two-dimensional and three-dimensional RFEM probabilistic analysis. Results indicated that the probability of failure based on 2D analysis is independent of the slope length, while the probability of failure based on 3D analysis depends on the slope length. In another study, Duncan [5] indicated that the conservativeness of 2D analysis is primarily a result of the selection of the most pessimistic section of a slope. However, the most pessimistic section of a slope may not be intuitive, especially for cases with random soils [6]. A recent study conducted by Ouyang and Liu [7] presents an effective approach for

* Corresponding author.
E-mail addresses: Ar.Kalantari@sutech.ac.ir (A.R. Kalantari), Johari@sutech.ac.ir (A. Johari), M.Zandpour@sutech.ac.ir (M. Zandpour), M.Kalantari@shirazu.ac.ir (M. Kalantari).

https://doi.org/10.1016/j.trgeo.2023.100933
Received 4 October 2022; Received in revised form 28 December 2022; Accepted 5 January 2023
Available online 14 January 2023

model updating that combines conditional random field with the Bayesian updating structural reliability methods algorithm to integrate multi-type observations. The results indicated that the proposed approach can update the probability distribution of spatially varying soil parameters and update the slope reliability using multi-type observations with reasonable calculation efficiency.

The soils are extremely variable within relatively short distances and rarely homogeneous. Spatial variability is an inherent characteristic of soil and an important issue for geotechnical studies. Several types of research have been conducted to evaluate the influence of soil heterogeneity on the reliability index (β), but the uncertainty of CSS has not been given enough consideration [8]. The CSS, which plays a key role in risk assessment and system reliability analysis of slopes, refers to the slip surface with the minimum FS. Determination of the CSS distribution hence has several applications are given as follows [9]. First, estimation of the key failure modes or representative slip surfaces, which are known as key inputs in system reliability or risk evolution. Second, estimation of the influential range (namely the area occupied by the CSS) to improve the efficiency of site investigation since the failure mechanism is significantly affected by soil parameters in this area. Third, providing useful information for inferring the correlation length of soil properties in back analyses as described in the work of Hicks and Spencer [10]. Albeit significant, the influence of spatial variability of soil properties on CSS distribution is rarely assessed. Jiang et al. [11] developed Monte Carlo Simulation (MCS)-based approach which facilitates the slope system reliability analysis using representative slip surfaces and multiple stochastic response surfaces in spatially variable soils. Sarma and Tan [12] developed a new method for estimating CSS within the framework of the LEM. Also, the method provided information on the critical acceleration for the calculation of seismic displacements. Sun et al. [13] presented a method in which the spline curve was used in conjunction with a genetic algorithm to identify the CSS. The major advantages of the presented method were its relatively low cost, ease of application, and shorter execution time. Xue and Gavin [14] presented a new method for extracting CSS and reliability index of soil slopes. The proposed method used a powerful genetic algorithm to find the CSS and reliability index simultaneously, taking less computation than other techniques.

Aside from computation time and cost, the FEM has well-known benefits, including (a) no special assumptions regarding the shape or location of the CSS are required; (b) information about deformations at working stress levels can be offered; and (c) boundary and loading conditions, complex material behavior, and problem geometry can be considered. The applicability of FEM for stochastic stability analysis of soil slopes has been investigated in several works, as in the following short note. Chen et al. [15] focused on combined Monte Carlo simulation and three-dimensional (3D) dynamic large-deformation finite-element analysis using the coupled Eulerian-Lagrangian method to investigate the whole runout process of landslide induced by the earthquake in spatially varying soil. The results showed that the calculated mean runout distance using the presented method is at least 16.1 % higher than that calculated using three-dimensional analysis. Liu et al. [16] investigated the coupled effect of strain softening and spatial variability on the occurrence, evolution, and runout behavior of landslides induced by seismic loads, using the 3D large-deformation finite-element method. The results show that both the strain-softening behavior and spatial variability of soil dramatically affect the sliding velocity and runout distance. Li et al. [17] presented an efficient Unconditional Random Finite Element Method (URFEM) for stability assessment by combining the URFEM with an advanced MCS technique. One of the superiorities of the presented method was that it quantifies the relative contributions of the slope failure risk at various probability levels to the total risk of the system. Cheng et al. [18] compared the locations of the CSS obtained by the LEM and FEM strength reduction method. In the case of homogenous, cohesive soil slopes with no friction angle, the results obtained from both methods were in good agreement with each other.

The available literature did not simultaneously take into account the real site data, borehole location, the uncertainty of surcharge load, and the uncertainty associated with soil properties. The goal of this study is to tackle these issues via stochastic analysis of the soil slope stability and CSS using a geostatistical conditional simulation system, which is the first of its kind. To do this, a real soil slope with fifteen boreholes was analyzed deterministically utilizing an elastoplastic finite element-based program coded in MATLAB. Fourteen arbitrary sections were considered to assess the influence of the borehole's location on the stability of soil slope, identify the most critical section, and eliminating the drawbacks of the two-dimensional analysis in determining the most pessimistic section of a slope that may not be intuitively clear. Then, a reliability assessment was done by employing the URFEM and Conditional Random Finite Element Method (CRFEM) by considering efficient soil properties and surcharge load as a stochastic parameter. Finally, the reliability characteristics and variations of the CSS for different simulation methods (i.e., unconditional and conditional) are compared, and the effect of different soil parameters on the CSS variation is investigated.

Methodology for stochastic analysis

In the current study, stochastic analysis of CSS and stability of soil slopes is presented using geostatistical conditional simulation. To address these issues, the geostatistical approach is implemented in FEM to take the boreholes' location and soil heterogeneity into account. For this purpose, effective parameters of soil, which are identified from sensitivity analysis, are modeled as stochastic parameters. A brief explanation of the selected methodology is described in the respective subsections.

Unconditional simulation

The soil properties are spatial variables and vary from one point in the field to another. This leads to the necessity of representing the soil parameters as characterized by random fields. The spatial variability of soil properties can be modeled using the theory of random fields. On the other hand, the values of a soil parameter in different parts of a field are correlated with each other. The spatial correlation of soil parameters can be characterized by auto-correlation [19]. In this research, the 2-D form of the Markov correlation function was used as follows:

$$\rho(x,x') = exp\left(-\frac{|x-x'|}{l_x} - \frac{|y-y'|}{l_y}\right) \tag{1}$$

where x and x' are spatial coordinates, l_x and l_y are autocorrelation lengths in horizontal and vertical directions, respectively. Due to the significant influence of the autocorrelation lengths on the stability of geotechnical problems, it would be more appropriate to evaluate them from known data [20–22]. The sample autocorrelation function (ACF) can be a simple and useful tool for this purpose. The ACF is the graph of the sample autocorrelation at lag k, r_k, for lags k = 0, 1, 2, …, m, where m is the maximum number of lags allowed for obtaining reliable estimates. The r_k is defined as follows [23]:

Table 1
Theoretical autocorrelation functions used to determine the autocorrelation lengths.

Model No.	ACF function	Autocorrelation lengths
1	$\rho_{\Delta z} = \begin{cases} 1-\dfrac{\lvert\Delta z\rvert}{a} & for\,\lvert\Delta z\rvert \leqslant a \\ 0 & for\,\lvert\Delta z\rvert \geqslant a \end{cases}$	a
2	$\rho_{\Delta z} = e^{-\lvert\Delta z\rvert/b}$	$2b$
3	$\rho_{\Delta z} = e^{-(\lvert\Delta z\rvert/c)^2}$	$\sqrt{\pi}c$
4	$\rho_{\Delta z} = e^{-\lvert\Delta z\rvert/d}(1+\dfrac{\lvert\Delta z\rvert}{d})$	$4d$

$$r_k = \frac{\sum_{i=1}^{N-k}(X_i - \overline{X})(X_{i+k} - \overline{X})}{\sum_{i=1}^{N}(X_i - \overline{X})^2} \tag{2}$$

where X_i and X_{i+k} are the values of the variable at points i and $i+k$ respectively; and $\overline{X}$ is the mean value of the variable. Vanmarcke [24] suggested that autocorrelation lengths can be determined by fitting one of the models to the sample ACF, as given in Table 1, where Δz is the depth interval.

To combine random field theory with the FEM, it is necessary to assign a specific value to each element by a method called discretization of a random field. There are several methods to discretize a random field in the literature [25]. In this research, the covariance matrix decomposition technique [26] was utilized for this purpose using the following steps:

1. Estimation of the correlation matrix $\rho(x_1,x_2)$, using Eq. (1).
2. Obtaining the Cholesky decomposition of $\rho(x_1,x_2)$ by the lower triangular matrix A as follows:

$$AA^T = \rho(x_1, x_2) \tag{3}$$

3. Define two independent standard normally distributed random fields from the following equation:

$$G_i = AZ_i (i = 1, 2) \tag{4}$$

Where Z is the standard normal distribution function.

4. If two random variables correlate, then it is essential to estimate the correlated G_i using steps 4 and 5:

$$LL^T = \begin{bmatrix} 1 & \rho_{c,\varphi} \\ \rho_{c,\varphi} & 1 \end{bmatrix} \tag{5}$$

5. Estimating the cross-correlated random c and φ fields as follow:

$$\begin{Bmatrix} G_c \\ G_\varphi \end{Bmatrix} = \begin{bmatrix} L_{11} & 0.0 \\ L_{21} & L_{22} \end{bmatrix} \begin{Bmatrix} G_1 \\ G_2 \end{Bmatrix} \tag{6}$$

The G_c and G_φ should be utilized instead of G_1 and G_2 in Eq. (7).

6. Using mean and standard deviation for each random parameter, the realization can be carried out as follow:

$$X_i = \mu_x(x_i) + \sigma_x(x_i) G_i \tag{7}$$

Where x_i is a correlated parameter randomly.

Conditional simulation

Assessment of uncertainty is essential for topics that have considerable interaction with soil particles. In geotechnical applications, it is common to evaluate the soil parameters using the limited data extracted from boreholes. Unconditional random fields discard these data and will cause large variability in the stability statement. However, in some conditional simulations, the boreholes' data are directly mapped into the analysis section without implementing the location of the samples, which can either overestimate or underestimate the stability of the slope. The geostatistical technique offers a framework to incorporate the known data and model the soil uncertainty [27]. The key purpose of implementing this technique is to evaluate the soil properties between boreholes' samples, which generally includes samples that represent a small part of the domain [28].

The estimation of correlation between samples along a specific orientation is vital in geostatistics analysis, which is usually estimated by the semivariogram. The experimental semivariogram for a set of data Z(xi), i = 1,2,… can be defined as [29]:

$$\gamma_{jj}(h) = \frac{1}{2N_{jj}(h)} = \sum_{i=1}^{N} \left[Z_j(X_i) - Z_j(X_i + h)\right]^2 \tag{8}$$

where $N_{jj}(h)$ is the number of pairs of data points separated by the particular lag vector h. The cross-semivariogram for random functions $Z_j(x)$ and $Z_k(x)$, which described the spatial dependence between cross-correlated variables, can be expressed as follow:

$$\gamma_{jk}(h) = \frac{1}{2N_{jk}(h)} = \sum_{i=1}^{N} \left\{ \left[Z_j(X_i) - Z_j(X_i + h)\right] \left[Z_k(X_i) - Z_k(X_i + h)\right] \right\} \tag{9}$$

where $N_{jk}(h)$ is the number of pairs of data points, separated by h, which have measured values of both random functions $Z_j(x)$ and $Z_k(x)$.

The geostatistical interpolation technique is known as kriging. It is often preferred due to its accuracy and efficiency and is regarded as a univariate geostatistical tool to estimate an unknown value at a particular location. For an unknown field point x_0, the ordinary kriging estimator $Z^*(x_0)$ based on the known data $Z(x_i)$, i = 1, 2…, N is defined as the linear unbiased estimator [30,31]:

$$Z^*(x_0) = \sum_{i=1}^{N} \lambda_i Z(x_i) \tag{10}$$

$$\sigma^2_{OK} = \beta_{OK} - \gamma(x_0, x_0) + \sum_{i=1}^{N} \lambda_i \gamma(x_0, x_i) \tag{11}$$

where Z* and σ_{ok} are the mean and standard deviation values in geostatistical estimation by the ordinary kriging, respectively; $Z(x_i)$, i = 1, 2…, N has known values of the parameter (for instance, unit weight); λ and β_{OK} are the ordinary kriging coefficient and the Lagrangian parameter, respectively which are as follows:

$$\begin{bmatrix} \lambda_1 \\ \lambda_1 \\ \vdots \\ \lambda_N \\ \beta_{OK} \end{bmatrix} = \begin{bmatrix} \gamma_{(x_1,x_1)} & \gamma_{(x_1,x_2)} & \cdots & \gamma_{(x_1,x_N)} & 1 \\ \gamma_{(x_2,x_1)} & \gamma_{(x_2,x_2)} & \cdots & \gamma_{(x_2,x_N)} & 1 \\ \vdots & \vdots & \ddots & \vdots & \vdots \\ \gamma_{(x_N,x_1)} & \gamma_{(x_N,x_2)} & \cdots & \gamma_{(x_N,x_N)} & 1 \\ 1 & 1 & \cdots & 1 & 0 \end{bmatrix}^T \begin{bmatrix} \gamma_{(x_0,x_1)} \\ \gamma_{(x_0,x_2)} \\ \vdots \\ \gamma_{(x_0,x_N)} \\ 1 \end{bmatrix} \tag{12}$$

here $\gamma(x_i,x_j)$, i,j = 1,2,.., N is the semivariogram between known points, and $\gamma(x_0,x_i)$, i = 1,2,.., N is the semivariogram between known points and unknown point which are expressed as follows:

$$\gamma(x_0, x_i) = C_0 + C\left[\left(\frac{h}{a}\right)\right] \tag{13}$$

$$a = \sqrt{A_1^2[cos^2(\theta - \varphi)] + A_2^2[cos^2(\theta - \varphi)]} \tag{14}$$

where h and c are the distance between two points and the structural variance, respectively. a and c_0 are the range and the nugget, respectively; θ and φ are the angles corresponding to the maximum parameter changes and the angles between pairs of points relative to the vertical direction, respectively. A_1 and A_2 are the larger effective length and smaller effective length, respectively of the linear semivariogram model.

A multivariate geostatistical approach (i.e., Cokriging) is performed to calculate two or more co-regionalized variables (i.e., regionalized variables that show cross-correlation). The real advantage of Cokriging is to reduce calculation variances where one or more of the regionalized variables (i.e., random variables with space coordinates) are "undersampled" and correlated with each other. Undersampling refers to a situation in which the number of the primary variable to be evaluated (e.g., soil shear strength) is less than the others (e.g., soil water content), usually at a subset of the sampling points. Generally, between V correlated variables, the linear ordinary cokriging estimator for variable u at an unknown field point x_0 is [30,31]:

$$Z_x^*(x_0) = \sum_{l=1}^{V} \sum_{i=1}^{n_l} \lambda_{il} Z_i(x_i) \tag{15}$$

$$\sigma^2_{CK} = \sum_{j=1}^{nl} \lambda_{jl} \gamma(x_j, x_0) + \Psi x - \gamma_{xx}(x_0, x_0) \tag{16}$$

here, Z_x^* and σ_{Ck} are the mean and standard deviation values in

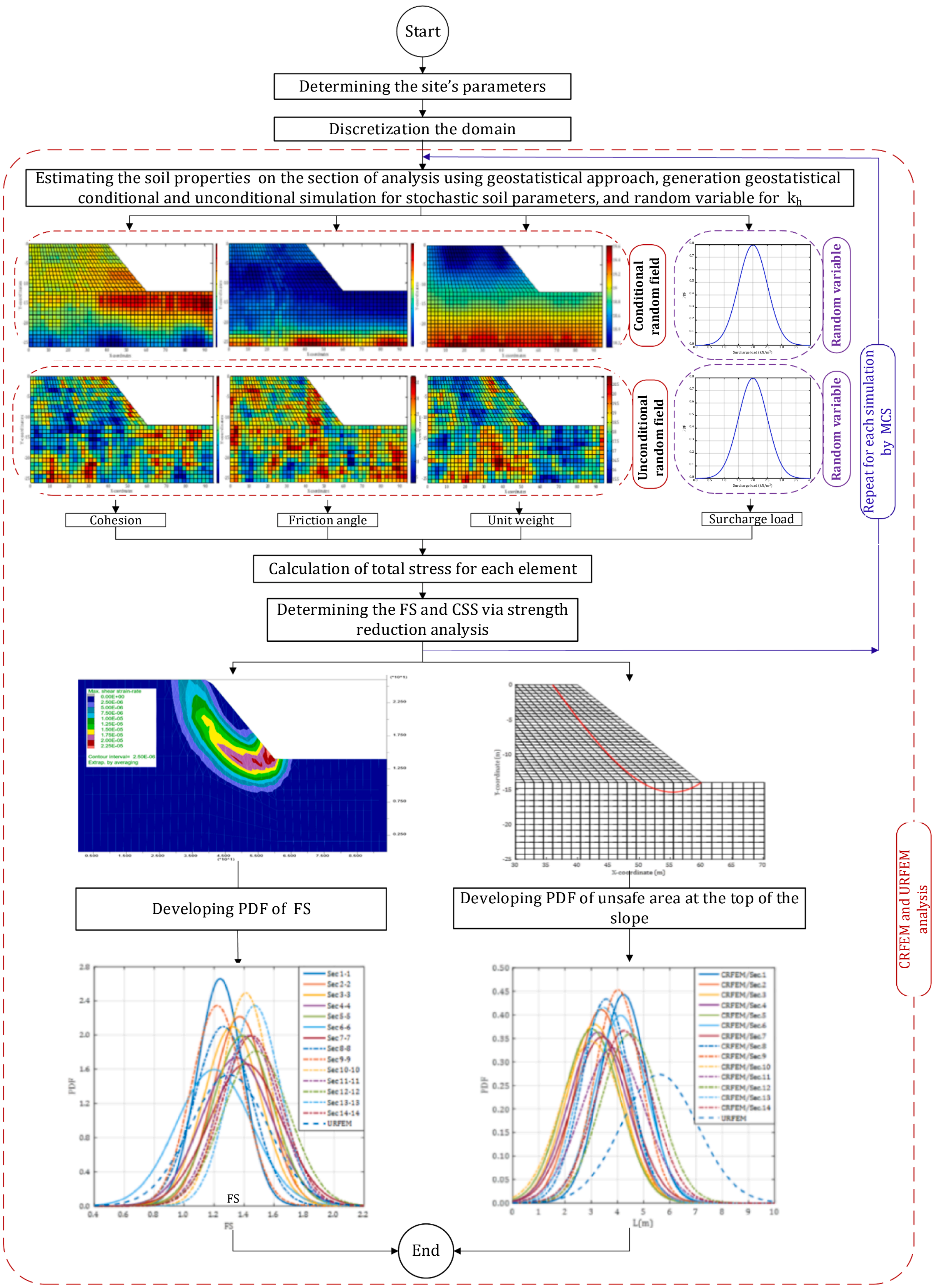

Fig. 1. Flowchart of obtaining the CSS of a slope by RFEM and GFEM.

geostatistical estimation by the ordinary cokriging, respectively; Z (x_i) is the known value of the parameter (for instance, cohesion); λ and Ψ_x are the ordinary cokriging coefficient and the Lagrange multipliers, respectively which are as follows:

$$\begin{bmatrix} \lambda_x^1 \\ \lambda_x^2 \\ \vdots \\ \lambda_{n_x x} \\ \lambda_y^1 \\ \lambda_y^2 \\ \vdots \\ \lambda_{n_y y} \\ \Psi_x \\ \Psi_y \end{bmatrix} = \begin{bmatrix} & & 1 & 0 \\ \gamma_{xx}^t & \gamma_{xy}^t & 1 & 0 \\ & & \vdots & \vdots \\ & & 1 & 0 \\ & & 0 & 1 \\ \gamma_{yx}^t & \gamma_{yy}^t & 0 & 1 \\ & & \vdots & \vdots \\ & & 0 & 1 \\ 11....1 & 00....0 & 0 & 0 \\ 00....0 & 11....1 & 0 & 0 \end{bmatrix}^T \begin{bmatrix} d_{xx} \\ d_{xy} \\ 1 \\ 0 \end{bmatrix} \tag{17}$$

where x and y are two variables of parameters in the geostatistical analysis (for instance, cohesion and friction angle); $\gamma^t{}_{xy}$ interprets a semivariograms matrix (containing cross-semivariograms where x ≠ y) between sampling points in a neighborhood, that these parameters are denoted as follows:

$$\gamma_{xy}^t = \begin{bmatrix} \gamma_{xy}(x_1, x_1) & \gamma_{xy}(x_1, x_2) & \cdots & \gamma_{xy}(x_1, x_{ny}) \\ \gamma_{xy}(x_2, x_1) & \gamma_{xy}(x_2, x_2) & \cdots & \gamma_{xy}(x_2, x_{ny}) \\ \vdots & \vdots & \ddots & \vdots \\ \gamma_{xy}(x_{nx}, x_1) & \gamma_{xy}(x_{nx}, x_2) & \cdots & \gamma_{xy}(x_{nx}, x_{ny}) \end{bmatrix} \tag{18}$$

$$d_{xx} = \begin{bmatrix} \gamma_{xx}(x_0, x_1) \\ \gamma_{xx}(x_0, x_2) \\ \vdots \\ \gamma_{xx}(x_0, x_{nx}) \end{bmatrix} \tag{19}$$

$$d_{xy} = \begin{bmatrix} \gamma_{xy}(x_0, x_1) \\ \gamma_{xy}(x_0, x_2) \\ \vdots \\ \gamma_{xy}(x_0, x_{ny}) \end{bmatrix} \tag{20}$$

here, d_{xx} and d_{xy} are semivariograms vectors for variable x; γ_{xx} and γ_{xy} are the direct and cross semivariogram, respectively, and both of them are exponential models which and defined as follows:

$$\gamma(x_i, x_n) = C_0 + C\left[1 - exp\left(\frac{-h}{a}\right)\right] \tag{21}$$

Execution process of reliability analysis

In previous parts, the processes of generating conditional and unconditional simulations were described. The principal emphasis of this part is on the implementation of the presented method for the stochastic stability assessment of soil slopes. The execution process is schematically demonstrated in Fig. 1 and can be defined as follows:

(1) Estimating the soil properties through the field and laboratory tests
(2) Discretization of the geometry

(3) Calculating soil properties on the unsampled levels and all levels of mapped boreholes utilizing the geostatistical approach.
(4) Conducting conditional simulation for soil parameters selected via sensitivity analysis.
(5) Creating a random variable for surcharge load.
(6) Estimating the total stress and the shear strength for each element of the soil.
(7) Calculating the FS and CSS via strength reduction analysis.

Fig. 2. Aerial view of the studied soil slope.

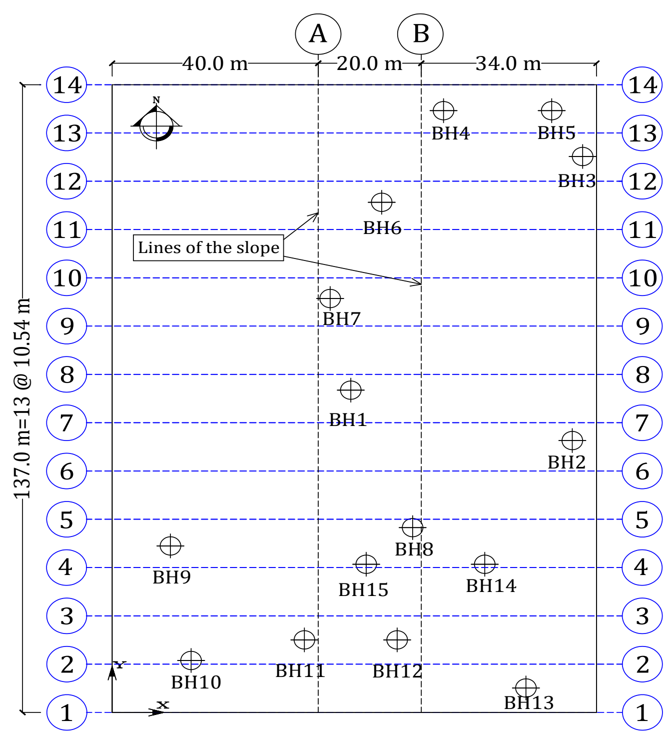

Fig. 3. Relative location of the boreholes and sections used in the analysis.

(8) Obtaining the reliability index and CSS distribution by repeating steps (2) to (6) for the optimal number of realizations.

Case study

In this section, a real soil slope is considered to evaluate the efficiency of the proposed method for stochastic stability and CSS distribution assessment. For this purpose, deterministic slope stability analyses are pursued by stochastic analysis of slope stability and CSS.

Table 2
The coordinates and depth of the boreholes.

BH.	1	2	3	4	5	6	7	8	9	10	11	12	13	14	15
X coordinate(m)	46.0	89.0	91.0	64.0	85.0	52.0	42.0	58.0	11.0	15.0	37.0	55.0	80.0	72.0	49.0
Y coordinate(m)	71.0	60.0	122.0	132.0	132.0	112.0	91.0	41.0	37.0	12.0	16.5	16.5	6.0	33.0	33.0
Depth(m)	26.0	26.0	25.0	25.0	26.0	25.0	26.0	25.0	26.0	25.0	26.0	25.0	26.0	25.0	25.0

Table 3
Geotechnical data of the site from the boreholes.

BH.		1	2	3	4	5	6	7	8	9	10	11	12	13	14	15
c (kN/m^2)	Min.	2.0	15.0	11.0	7.0	10.0	13.0	13.0	15.0	9.0	13.0	10.0	13.0	4.0	27.0	10.0
	Max.	14.0	22.0	30.0	30.0	19.0	27.0	18.0	30.0	10.0	30.0	14.0	32.0	20.0	30.0	30.0
ϕ (Deg.)	Min.	24.0	19.0	21.0	19.0	24.0	19.0	20.0	17.0	15.0	23.0	23.0	18.0	12.0	18.0	21.0
	Max.	37.0	25.0	38.0	37.0	27.0	38.0	38.0	33.0	29.0	33.0	25.0	37.0	35.0	24.0	38.0
γ (kN/m^3)	Min.	16.8	16.8	17.1	16.7	16.9	16.8	17.1	16.9	16.9	16.9	16.9	16.8	16.6	16.8	16.8
	Max.	20.5	17.8	20.4	20.2	19.8	20.2	20.4	17.7	20.5	19.8	20.6	20.4	20.6	17.2	20.5

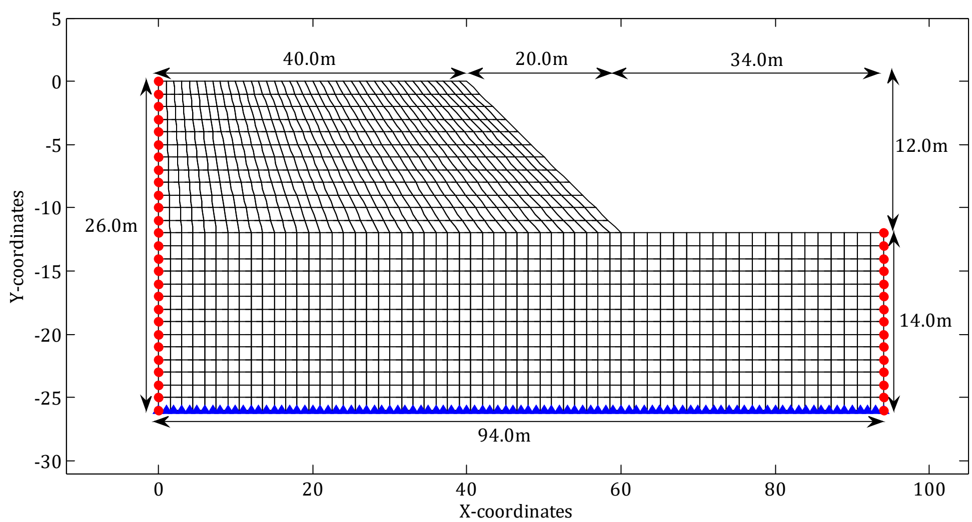

Fig. 4. The geometry of the modeled slope, finite element discretization, and boundary conditions.

Then, the results of CRFEM and URFEM were compared to assess the influence of conditional random field on the CSS and reliability index. Finally, the influence of different soil parameters on the location and scale of the CSS was investigated.

The site characterization and geotechnical soil properties

The actual case study employed in this paper is situated in Shiraz, located in southwest Iran, as depicted in Fig. 2. To determine soil properties, fifteen boreholes up to the depth of 26.0 m are drilled, as illustrated in Fig. 3 and tabulated in Table 2. For all soil samples, the textural and mechanical properties are obtained through field and laboratory tests, of which some of the most important are listed in Table 3. According to laboratory and boreholes data, the soil was normally consolidated silty clay and the groundwater level was below 26.0 m. One of the main aims of selecting the site was that the whole domain of the soil slope satisfies the generalized plane strain conditions.

Development and verification of a coded program

In this research, a finite element–based program is coded in MATLAB for the stability analysis of soil slope utilizing eight-node quadrilateral elements. The program is developed for the 2D plane strain analysis of elastic-perfect plastic with a Mohr-Coulomb yield criterion. The bottom boundary was considered fully restrained, while others were restrained horizontally. The general conditions of the model, such as its geometry, finite element mesh, and boundary conditions, are illustrated in Fig. 4. Also, the soil parameters implemented in the deterministic analysis and the related CSS are shown in Table 4 and Fig. 5, respectively. An identical model was used for verifying the coded program using the finite difference software package FLAC 7.0. Comparisons of FS and maximum displacement obtained from both methods are given in Table 5. The shear strain rate contour extracted from Flac 7.0, which is commonly known as the sliding zone [16], is illustrated in Fig. 6.

Table 4
The selected soil parameters used for deterministic analysis.

Soil parameters	c (kN/m^2)	ϕ (Deg.)	γ (kN/m^3)	E(kN/m^2)	υ
Value	15.0	20.0	20.0	3.5e4	0.3

Stochastic analysis

The stochastic stability analysis of the presented case study is taken into account in this section within the following subsections. Firstly, the selection of effective parameters of the soil that significantly influence the stability of the slope is offered. Secondly, the URFEM and CRFEM are presented to assess the influence of conditional simulation on the reliability index and CSS. Finally, the sensitivity analysis is presented to calculate the required number of simulations.

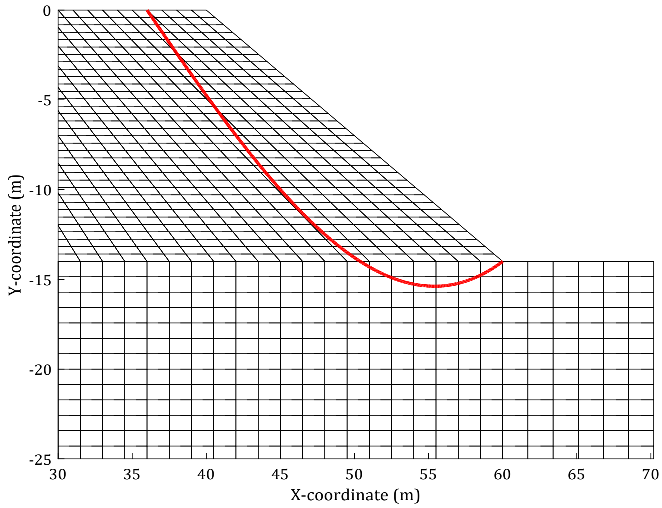

Fig. 5. The CSS obtained from the deterministic analysis.

Table 5
Comparison of the results.

Method	FS	Maximum displacement (cm)
Proposed model	1.30	1.70
FLAC	1.24	1.59

Sensitivity analysis for determining effective soil parameters

The determination of the effective soil parameters is a necessary step before the stochastic analysis. To do this, a sensitivity analysis was conducted by increasing each parameter by 10 % while the other parameters were held constant. As shown in Table 6, the unit weight (γ), cohesion (c), and friction angle (φ) are the most important parameters on the FS, while Poisson's ratio (ν) and modulus of elasticity (E_S) have no significant effect on it.

Table 6
Determination of influent soil properties.

Input parameter	Change in FS (%) (%)
γ	6.8
c	5.2
φ	4.1
E_S	0.3
ν	0.2

Stochastic analysis by URFEM

The unconditional random fields were made for soil parameters that were determined by sensitivity analysis. The parameters were modeled within four standard deviations (σ) of difference from the mean (μ), using truncated normal probability distribution functions with the μ and σ tabulated in Table 7, extracted from boreholes data listed in Table 3. The correlation coefficient between cohesion and friction angle was considered $\rho_{c,\varphi}$ = -0.5 [32].

Due to the availability of sufficient soil data in a vertical direction, the l_y was estimated using the ACF, and single exponential curve model (i.e., model No.2 in Table 1) described in section 3.1. A typical sample of the ACF model for the soil parameters of BH.3 is illustrated in Fig. 7 and the fitting parameter values for all boreholes are presented in Table 8. According to the results, the l_y was considered 3.5 m as twice the mean value of parameter b obtained from boreholes, which was within the range of (0.1–7.2 m) estimated by various studies [33]. Furthermore, l_x was considered as 30 m since the horizontal correlation length is usually much larger, and its influence is much less important compared with the vertical correlation length [34].

The random field of different parameters in the typical realization is

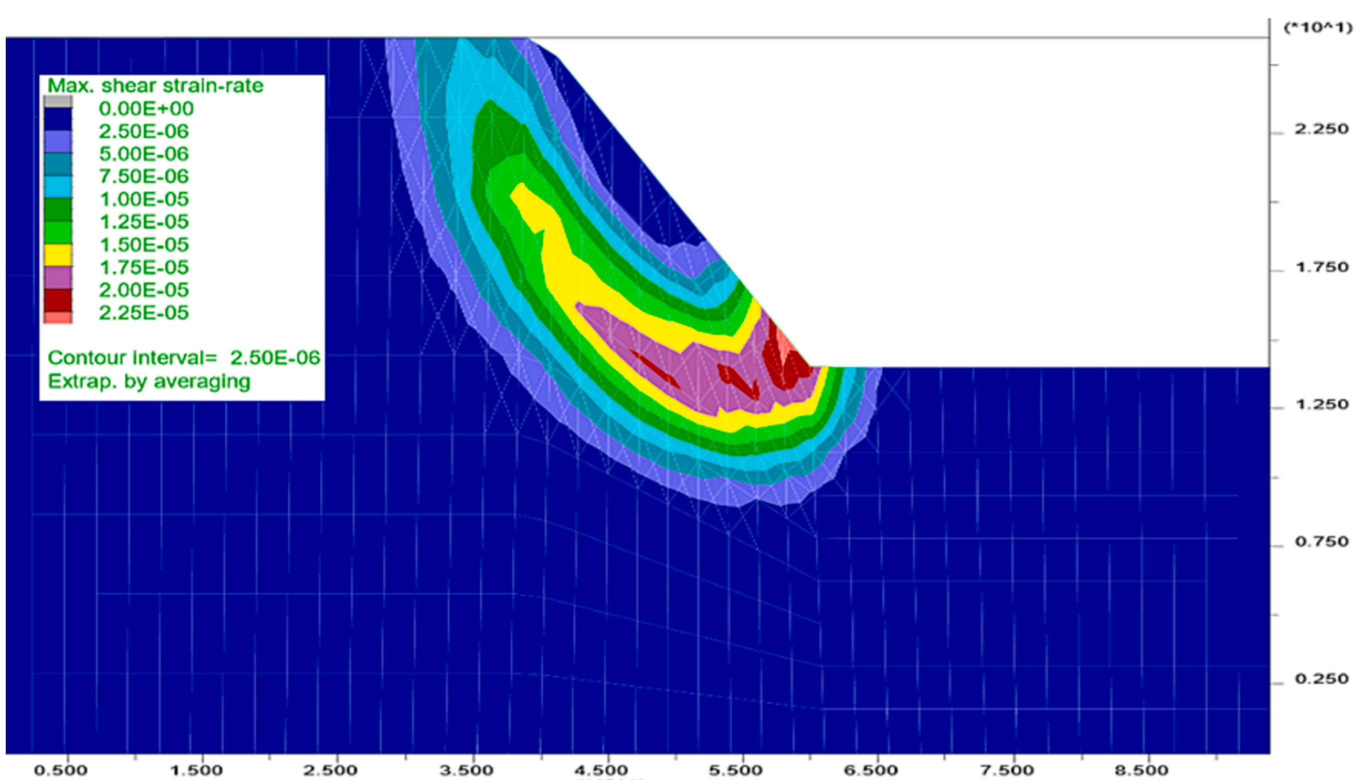

Fig. 6. The shear strain rate of a modeled slope estimated by FLAC.

Table 7
The stochastic parameters based on boreholes' data.

Soil parameters	c (kN/m^2)	ϕ (Deg.)	γ (kN/m^3)
Mean	15.15	20 0.07	17.98
STD	3.35	3.97	0.52

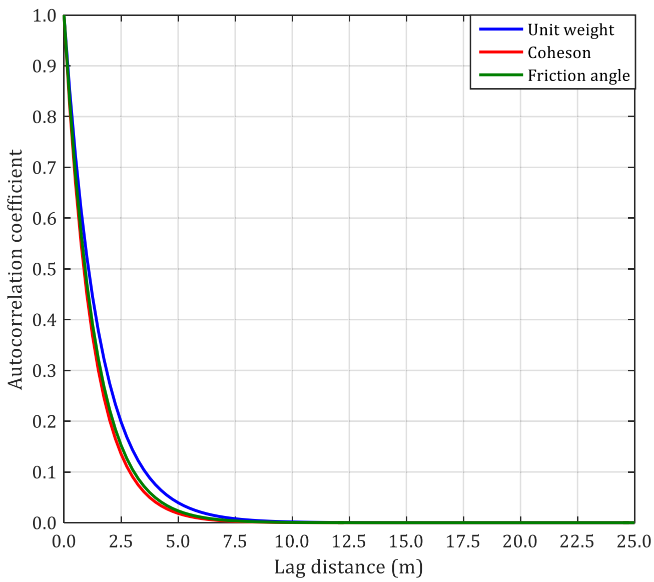

Fig. 7. Sensitivity analysis of the number of realizations.

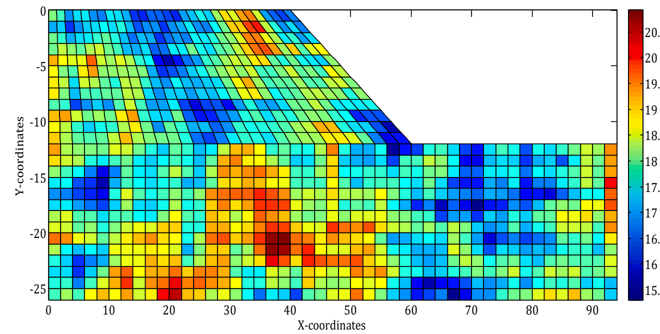

Fig. 8. The random field of unit weight in the typical realization(kN/m^3).

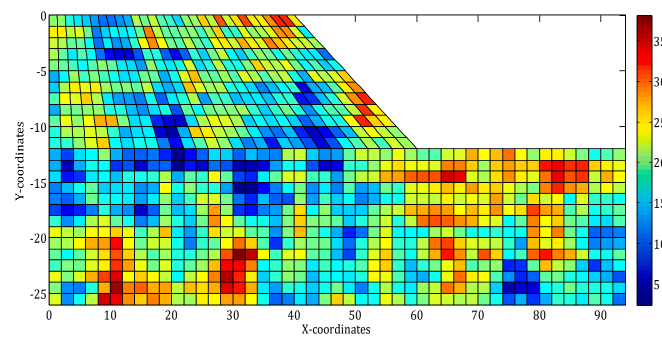

Fig. 9. The random field of cohesion in the typical realization (kN/m^2).

depicted in Figs. 8 to 10. Besides the soil parameters, the surcharge load, which has an important role in the stability and CSS distribution of soil slopes, was considered a random variable with a normal distribution, as illustrated in Fig. 11.

Stochastic analysis by CRFEM

The geostatistical method is applied to predict the fluctuation of soil properties between the boreholes data at specific locations. To provide this and to eliminate the drawbacks of unconditional simulation, such as the unconformity of measured values, the conditional simulation for selected parameters was made using the geostatistical method. Due to the dominant role of surcharge load in stability and location of CSS of soil slopes, it is considered a random variable with a normal distribution, as mentioned in the previous subsection and shown in Fig. 11. Also, to evaluate the influence of boreholes' location on CSS distribution and reliability characteristics, 14 arbitrary sections of analysis were considered as illustrated in Fig. 3.

At first, a regression analysis was carried out to identify the dependency of the stochastic parameters. According to the outcomes shown in Table 9, the cohesion and friction angle indicates a high dependency. Therefore, the Cokriging technique was applied to evaluate these parameters, and the others were evaluated by the Kriging technique. Since extracting the shear strength is much more costly and time-consuming than other soil properties, the shear strength data is limited. To tackle this problem, the Cokriging technique was applied to increase the interpolation efficiency without having to do more intense sampling.

Despite the URFEM analysis in which the correlation length is calculated from boreholes data, in the current technique, this factor is calculated by anisotropy semivariogram analysis. The semivariogram has the advantage of analyzing the spatial dependence between samples not only in the normal direction but also in an oblique direction, which can be regarded as the superiority of the geostatistical method. Since there are various anisotropic models for semivariogram (e.g., circular, spherical, and exponential), the residual sums of squares and coefficient of determination (R^2) methods were used to determine which model best fits the data. Based on the results, the exponential model was selected for the stochastic parameters in the current study.

To tackle the inadequacy of two-dimensional analysis for accurately representing the spatial variability of soil properties in the three-dimensional space the conditional estimation of soil parameters in this study is performed as follows:

- First, the unknown soil parameters of each depth are interpolated based on known data of other boreholes at the same depth using Kriging and Cokriging methods, as shown in an arbitrary borehole BH1 in Fig. 12.
- Then, the soil parameters at each level are estimated in the section of analysis based on the boreholes' location using Kriging and Cokriging methods, as shown in an arbitrary section 5–5 for BH'9 in Fig. 13.

Table 8
Parameter b estimated from fitted model of boreholes.

Parameters	$b_{(BH.1)}$	$b_{(BH.2)}$	$b_{(BH.3)}$	$b_{(BH.4)}$	$b_{(BH.5)}$	$b_{(BH.6)}$	$b_{(BH.7)}$	$b_{(BH.8)}$	$b_{(BH.9)}$	$b_{(BH.10)}$	$b_{(BH.11)}$	$b_{(BH.12)}$	$b_{(BH.13)}$	$b_{(BH.14)}$	$b_{(BH.15)}$
Unit weight	1.50	1.44	1.54	1.50	1.52	1.37	1.40	1.41	1.49	1.44	1.53	1.54	1.52	1.63	1.67
Friction angle	1.38	1.33	1.25	1.37	1.45	1.41	1.43	1.45	1.61	1.60	1.65	1.57	1.59	1.65	1.69
Cohesion	1.45	1.41	1.33	1.39	1.53	2.47	1.45	1.52	1.64	1.65	1.68	1.66	1.66	1.70	1.70

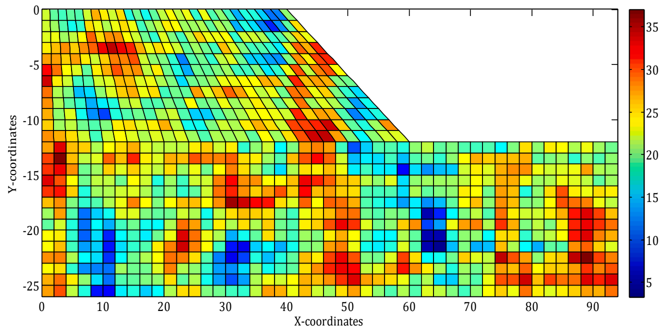

Fig. 10. The random field of friction angle in the typical realization (Deg.).

- Finally, the estimated data in the previous step were utilized for estimating the soil properties of all elements in the section of analysis using the Kriging and Cokriging methods. To do this, only a certain number of near neighbors' known data, which is required to be within a particular geographic area (e.g., circular or elliptical) around the location, are used. Whereas in geotechnical problems, the scale of fluctuation in the y-direction is less than in the x-direction, a horizontal ellipse was utilized in this research as a geographic area.

The conditional simulation of soil parameters through one realization for arbitrary sections 3–3 are presented in Figs. 14 to 16. The figures imply the inverse correlation between friction angle and cohesion. Besides, the simulated values match the boreholes data, which can be accounted for the differences among the unconditional and conditional random fields.

Calculating the essential number of MCS runs

The obtained value of FS, which gives a quantitative evaluation of stability, is generally less accurate because of the uncertainty involved in its assessment. To extract the Probability Density Function (PDF) of FS, the analysis was repeated as essential due to the acceptable accuracy of the outcomes. Recent research [35] used different parameters such as μ, σ, and the Coefficient of Variation (COV) to calculate the required number of simulations. In this study, a sensitivity analysis was performed using a COV of FS, which is defined as the ratio of the σ to the μ. Fig. 17 depicts the variations of COV with the number of MCS runs in

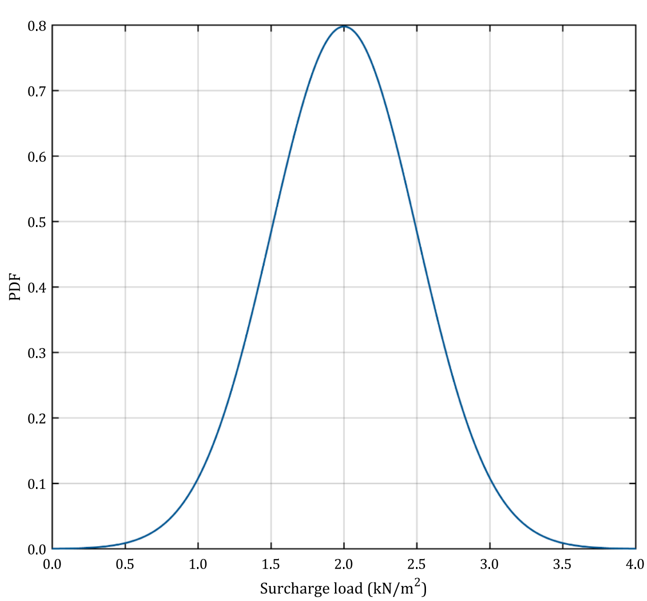

Fig. 11. The random variable of surcharge load (kN/m^2).

Table 9
Regression analysis of stochastic parameters.

Parameters	Unit weight	Friction angle	Cohesion
Unit weight	1.00	−0.48	0.42
Friction angle		1.00	−0.94
Cohesion			1.00

both URFEM and CRFEM analysis. The sufficient number of simulations was evaluated to be 500, and beyond it, no significant change occurred in the value of COVs.

Results and discussion

In this section, the results of the stochastic analysis of soil slope are presented in several subsections. First, the impact of conditional simulation and boreholes' location on reliability characteristics are evaluated. Then, the effect of conditional simulation on the shape and location of CSS is assessed by comparing the outcomes of CRFEM with the URFEM analysis. At last, the influence of different soil parameters on the variation of CSS is investigated.

Influence of conditional simulation and boreholes location on reliability characteristics

To assess the impact of the conditional simulation and boreholes location on reliability characteristics, the PDFs of FS extracted from URFEM and CRFEM in a different section of analysis are plotted in Fig. 18. The statistics and probabilistic characteristics of these PDFs for

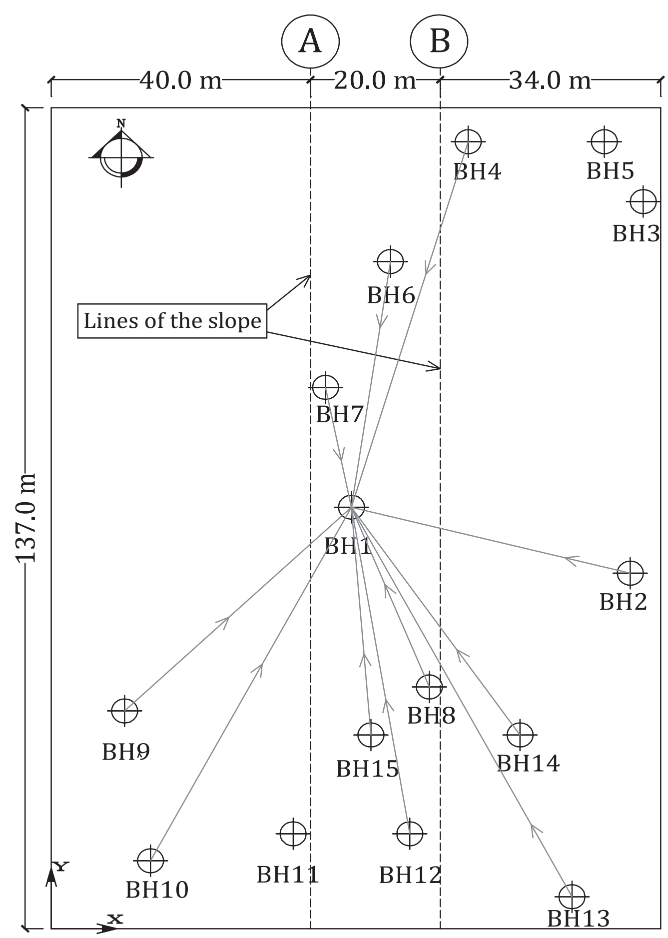

Fig. 12. Prediction of unknown soil parameters in each depth of an arbitrary borehole, BH1 (first step).

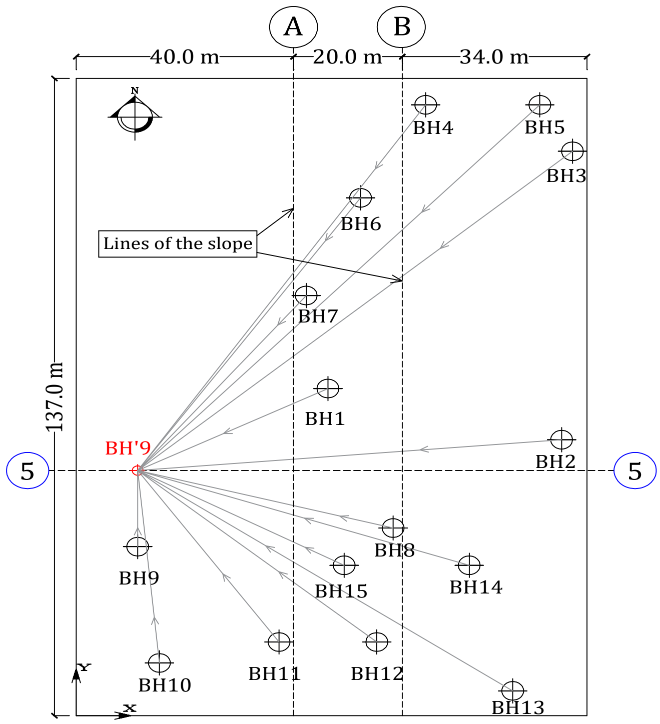

Fig. 13. Prediction of soil parameters in an arbitrary section 5–5 for virtual boreholes, BH'9 (second step).

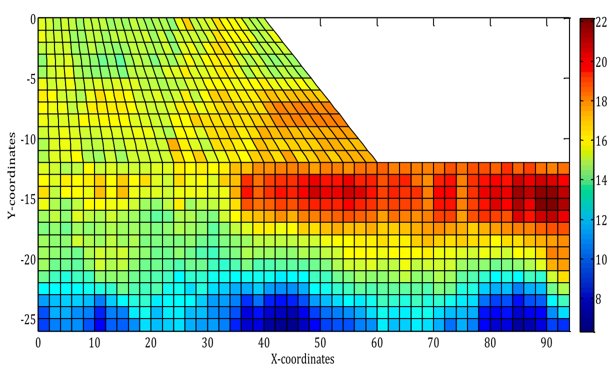

Fig. 14. The conditional random field of cohesion in the typical realization (kN/m^2).

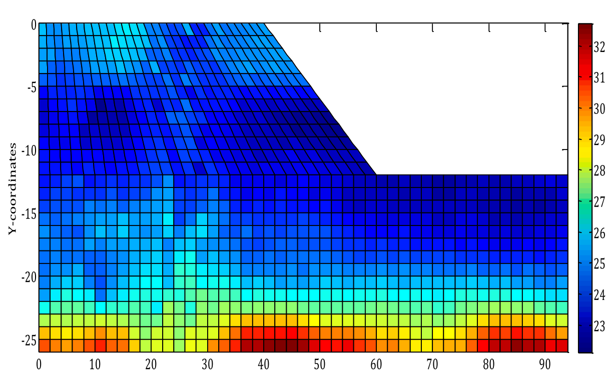

Fig. 15. The conditional random field of spatial variation for friction angle (Deg.).

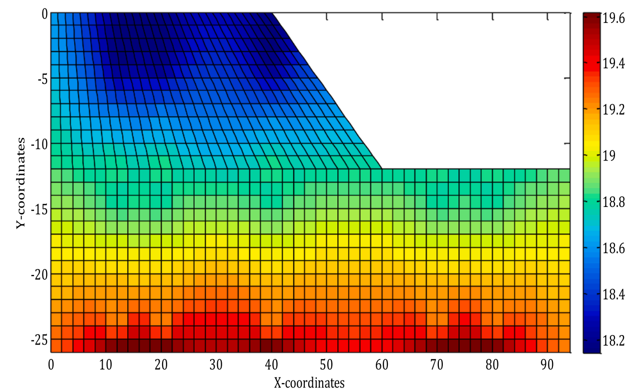

Fig. 16. The conditional random field of unit weight in the typical realization (kN/m^3).

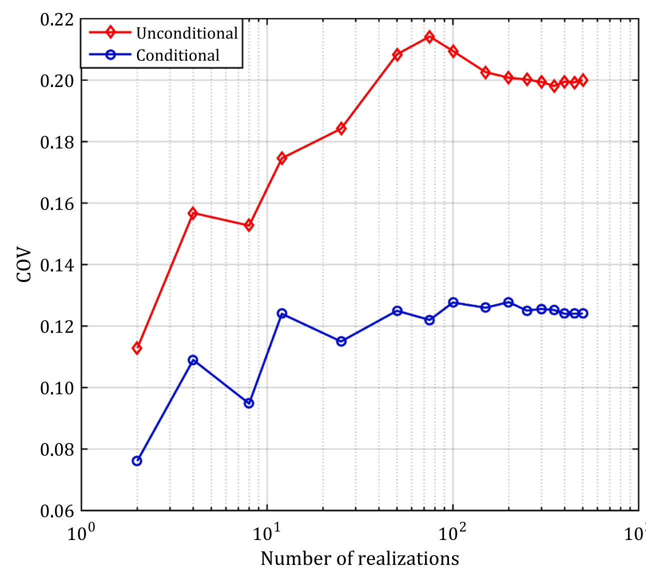

Fig. 17. Variation of COV with the number of realization.

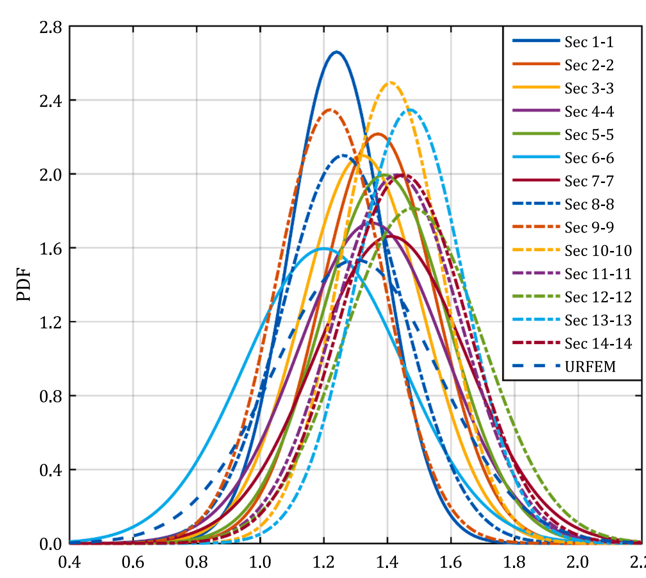

Fig. 18. The PDF of FS estimated by URFEM and CRFEM method.

Table 10
Comparison of the reliability characteristics obtained from CRFEM and URFEM analysis.

Method of analysis	Section	μ	σ	COV	β
CRFEM	1–1	1.24	0.15	0.12	1.60
	2–2	1.37	0.18	0.13	2.06
	3–3	1.32	0.19	0.14	1.68
	4–4	1.35	0.23	0.17	1.52
	5–5	1.39	0.20	0.14	1.95
	6–6	1.21	0.25	0.20	0.80
	7–7	1.41	0.24	0.17	1.71
	8–8	1.26	0.19	0.15	1.37
	9–9	1.22	0.17	0.14	1.29
	10–10	1.41	0.16	0.11	2.56
	11–11	1.43	0.20	0.14	2.15
	12–12	1.48	0.22	0.15	2.18
	13–13	1.47	0.17	0.12	2.76
URFEM	14–14	1.45	0.21	0.14	2.14
URFEM	–	1.30	0.27	0.21	1.154

the two methods of analysis are listed in Table 10. A comparison between reliability indices reveals that the conventional URFEM may underestimate or overestimate the reliability index while the CRFEM can correctly estimate the uncertainties and offer more dependable results. Also, compared to the URFEM, the PDFs obtained from CRFEM analysis have relatively small values of σ and relatively large values of μ. These considerable variations can cause a significant effect on the stability of soil slope by shifting its performance level from a risky zone to the safer one, according to the U.S. Army Corps of Engineers [36], which can be considered as an aim of reliability analysis [37,38].

Influence of conditional simulation and boreholes location on the variation of CSS

The advantage of FEM over other methods of stability assessment is determining the CSS without requiring the prior assumption. To assess the effect of conditional simulation on a critical slip surface's shape and position, 500 realizations are created by URFEM and CRFEM analysis. Fig. 19(a) and 19(b) plot the variation of CSS in the URFEM and CRFEM (section 5–5) analysis, respectively. These figures imply the fact that the unsafe zone at the top of the slope (L), as summarized in Table 11 for both methods of analysis, decreases by utilizing conditional simulation. Moreover, taking the boreholes data in stability assessment by using the conditional simulation results in a less influential range with lower μ and

Table 11
Comparison of the statistical parameters of the L from CRFEM and URFEM analysis.

Method of analysis	Section	μ	σ	COV
CRFEM	1–1	4.23	1.25	0.30
	2–2	3.37	1.27	0.38
	3–3	3.12	1.30	0.42
	4–4	3.25	1.33	0.41
	5–5	3.02	1.32	0.44
	6–6	4.12	1.30	0.32
	7–7	3.41	1.34	0.39
	8–8	3.56	1.29	0.36
	9–9	4.02	1.27	0.32
	10–10	3.01	1.26	0.42
	11–11	3.83	1.30	0.34
	12–12	4.49	1.31	0.29
	13–13	3.46	1.26	0.36
URFEM	14–14	4.25	1.29	0.30
URFEM	–	5.60	2.26	0.40

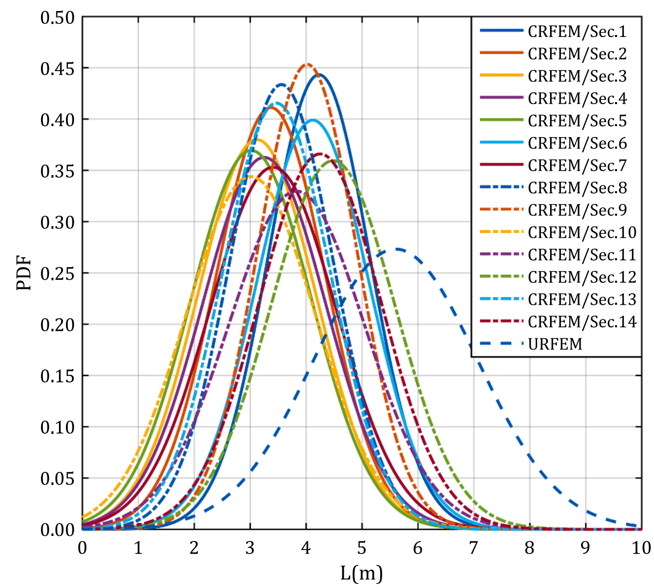

Fig. 20. The PDF of L estimated by URFEM and CRFEM method.

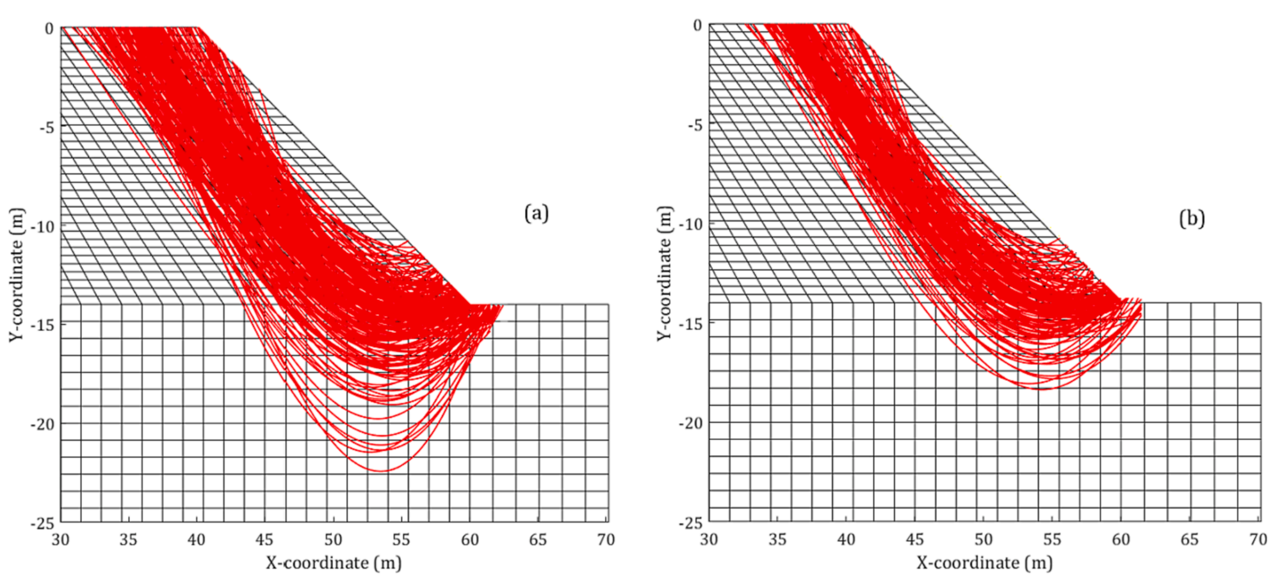

Fig. 19. Uncertainties of the CSS extracted from; (a) URFEM analysis, and (b) CRFEM analysis.

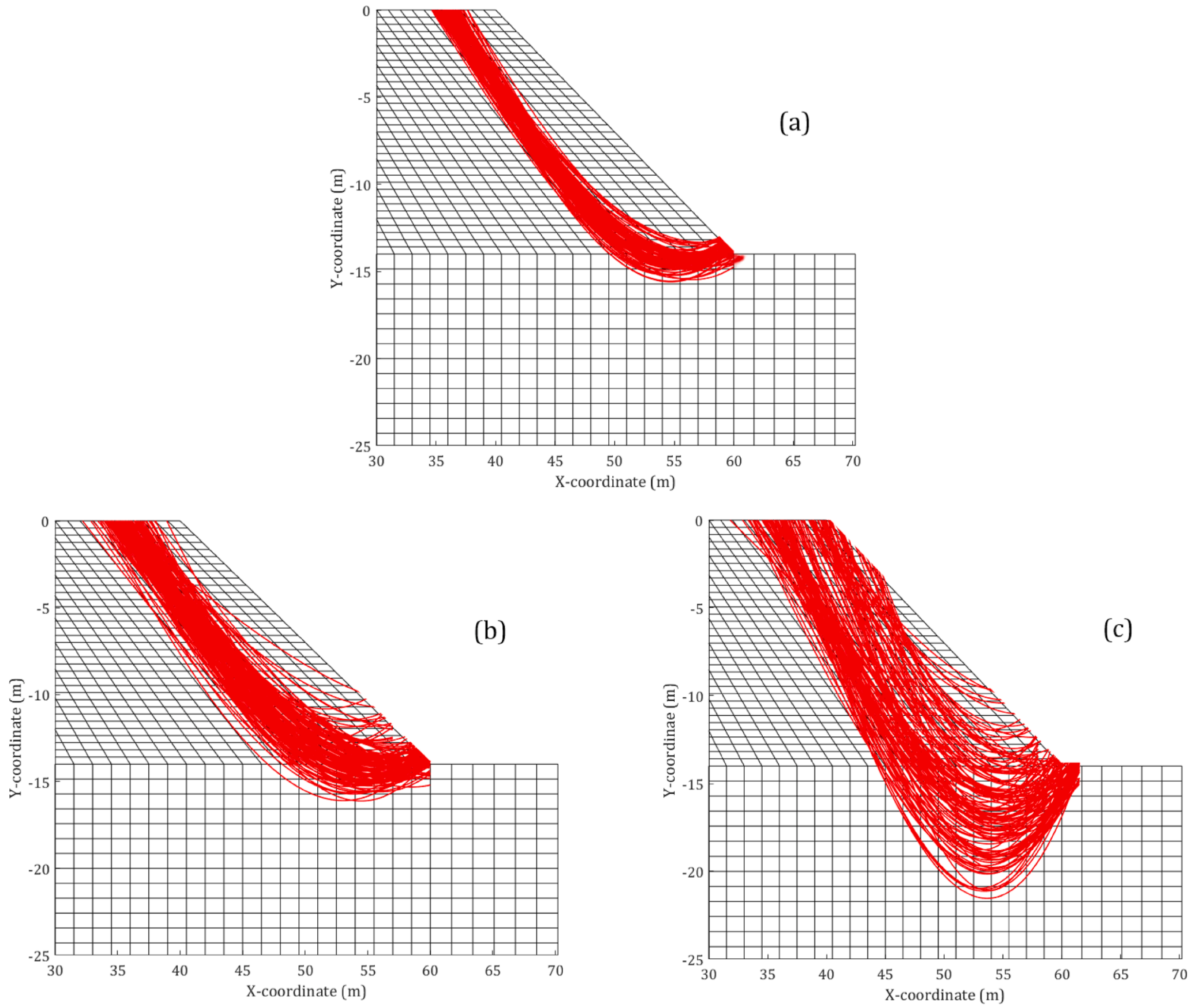

Fig. 21. The CSS distribution for spatial variability of different soil parameters (a) unit weight; (b) friction angle; (c) cohesion.

σ, which reflects less uncertainty in the CSS. Fig. 20 shows the PDFs of the L extracted by two methods of simulation. In line with the results, by taking the conditional simulation into account, the mean and standard deviation of L decreased by 20–39 % and 8–31 %, respectively.

Influence of different soil parameters on the variation of CSS

In the current subsection, the influence of spatial variability of different soil parameters on CSS distribution is evaluated. To do this, stochastic analyses were conducted by considering the spatial variability of each effective soil parameter (i.e., cohesion, friction angle, and unit weight) while the other parameters were held constant. The variations of CSS for the three cases of soil spatial variability are plotted in Fig. 21(a-c).

As illustrated in Fig. 21(a), the CSS distribution is less affected by spatial variability of soil unit weight than others. In other words, the CSSs for the case with only spatially varying unit weight are located around the CSS of deterministic analysis, and no local failure occurred in this case. As indicated in previous studies [39,40], this phenomenon may attribute to a relatively small COV of unit weight compared to the other soil parameters. Fig. 21(b) show the CSS distributions for slopes with spatially varying friction angle. Compared with the case of spatially varying unit weight, this case has relatively large variation ranges of CSS. Despite the previous case (i.e., spatially varying unit weight), which can only produce the overall CSS, the CSS of this case consists of both local and overall. The local CSS refers to a CSS with an entry point or an exit point on the slope surface. As shown in Fig. 21(b), although the CSSs of this case contain a local type, all the CSSs have an entry point located at the top of the slope. In the last case, the variation of CSS for slope with spatially varying cohesion is presented in Fig. 21(c). As can be seen, this case has the largest variation ranges of CSS. Furthermore, the CSSs of this case consists of the overall and the local CSS which an entry point located either at the top or surface of the slope. This observation is different from the previous cases as plotted in Fig. 21(a) and (b), where only overall CSS happens or local CSS enters merely at the top of the slope.

The importance of identifying the CSS distribution lies in recognizing its role in reliability analyses of soil slopes which are rarely considered in most of the previous studies. One of the studies which considered the effects of soil parameters on the variation of CSS was presented by Qi and Li [40]. It was found that local CSS may contribute a large part to the probability of failure of a slope and should be well considered in system reliability analyses of slopes. Also, it showed that the local failures with entry points on the slope surface contribute 5.6 % of the failures, and ignoring them may lead to an overestimation of the reliability index.

Conclusions and recommendations

This article presents the reliability method for the evaluation of the stability and CSS distribution of soil slopes. The necessity for developing the proposed method arrived due to the lack of literature on the stochastic analysis of stability and CSS variation of soil slopes, considering the known data and its measured locations, conditional simulation, uncertainty of surcharge load, and soil heterogeneity. To do this, a real soil slope with fifteen 26 m depth boreholes was considered, and the soil properties were obtained from geotechnical site investigation and laboratory tests. The deterministic analysis was carried out using a FEM-based MATLAB code. After that, the analysis was performed stochastically by the URFEM and then by CRFEM to implement the known data and its measured location. Lastly, the reliability characteristics and CSS distribution of URFEM and fourteen sections of CRFEM analysis were obtained and compared. Based on numerical analysis, some conclusions are made below:

(1) The results for estimating the optimum number of simulations indicated that the 500 MCS runs are sufficient for the stability evaluation of soil slope. Moreover, it was revealed that the γ, c, and φ are the most effective soil parameters in the stochastic stability assessment of soil slopes.

(2) It was illustrated from the PDFs of FS that incorporating the sampled data and its location results in less distributed CSS that decreases the μ and σ of the unsafe zone at the top of the slope by 20–46 % and 40–45 %, respectively. Also, it improves the mean value of FS up to 14 % while decreasing the related standard deviation by 4 % to 40 %.

(3) Ignoring the soil heterogeneity or considering spatial variability with small COV can only produce an overall CSS. However, if the spatial variability of friction angle is considered, the CSS could be a local one with an entry point located at the top of a slope. In the case of spatially varied cohesion, the local CSS has entry points at the top of the slope's surface.

However, the proposed method evaluates the stochastic analysis of CSS and stability of soil slopes using geostatistical conditional simulation but extracting the overall reliability by combining the reliability indices of different sections via system reliability analysis and considering the effect of both correlation length and COV of soil parameters on CSS variation was not considered. Hence, further research is required to study the application of the proposed method in conjunction with the system reliability approach, such as the sequential compounding method.

CRediT authorship contribution statement

A.R. Kalantari: Writing – original draft, Formal analysis, Validation. **A. Johari:** Conceptualization, Methodology, Supervision. **M. Zandpour:** Software, Methodology, Investigation. **M. Kalantari:** Writing – review & editing, Project administration.

Declaration of Competing Interest

The authors declare that they have no known competing financial interests or personal relationships that could have appeared to influence the work reported in this paper.

Data availability

Data will be made available on request.

References

[1] Griffiths D, Fenton GA. Seepage beneath water retaining structures founded on spatially random soil. Geotechnique 1993;43:577–87.
[2] Wong FS. Slope reliability and response surface method. J Geotech Eng 1985;111(1):32–53.
[3] Ou-Yang JY, Li DQ, Tang XS, Liu Y. A patching algorithm for conditional random fields in modeling material properties. Comput Methods Appl Mech Eng 2021;377:113719.
[4] Griffiths DV, Huang J, Fenton GA. On the reliability of earth slopes in three dimensions. Proc Roy Soc A: Math, Phys Eng Sci 2009;465(2110):3145-3164.
[5] Duncan JM. Soil slope stability analysis. Landslides: Investigation and Mitigation. Transport Res Board Special Report 1996;247:337–71.
[6] Liu Y, Zhang W, Zhang L, Zhu Z, Hu J, Wei H. Probabilistic stability analyses of undrained slopes by 3D random fields and finite element methods. Geosci Front 2018;9(6):1657–64.
[7] Ouyang J, Liu Y. Model updating for slope stability assessment in spatially varying soil parameters using multi-type observations. Mech Syst Sig Process 2022;171:108906.
[8] Johari A, Fooladi H. Simulation of the conditional models of borehole's characteristics for slope reliability assessment. Transp Geotech 2022;35:100778. https://doi.org/10.1016/j.trgeo.2022.100778.
[9] Li L, Wang Y, Cao Z, Chu X. Risk de-aggregation and system reliability analysis of slope stability using representative slip surfaces. Comput Geotech 2013;53:95–105.
[10] Hicks MA, Spencer WA. Influence of heterogeneity on the reliability and failure of a long 3D slope. Comput Geotech 2010;37(7–8):948–55.
[11] Jiang SH, Li DQ, Cao ZJ, Zhou CB, Phoon KK. Efficient system reliability analysis of slope stability in spatially variable soils using Monte Carlo simulation. J Geotech Geoenviron Eng 2015;141(2):04014096.
[12] Sarma SK, Tan D. Determination of critical slip surface in slope analysis. Géotechnique 2006;56(8):539–50.
[13] Sun J, Li J, Liu Q. Search for critical slip surface in slope stability analysis by spline-based GA method. J Geotech Geoenviron Eng 2008;134(2):252–6.
[14] Xue JF, Gavin K. Simultaneous determination of critical slip surface and reliability index for slopes. J Geotech Geoenviron Eng 2007;133(7):878–86.
[15] Chen X, Li D, Tang X, Liu Y. A three-dimensional large-deformation random finite-element study of landslide runout considering spatially varying soil. Landslides 2021;18(9):3149–62.
[16] Liu Y, Chen X, Hu M. Three-dimensional large deformation modelling of landslides in spatially variable and strain-softening soils subjected to seismic loads. Can Geotech J (ja) 2022.
[17] Li DQ, Xiao T, Cao ZJ, Zhou CB, Zhang LM. Enhancement of random finite element method in reliability analysis and risk assessment of soil slopes using Subset Simulation. Landslides 2016;13(2):293–303.
[18] Cheng Y, Lansivaara T, Wei W. Two-dimensional slope stability analysis by limit equilibrium and strength reduction methods. Comput Geotech 2007;34(3):137–50.
[19] Kalantari AR, Johari A. System Reliability Analysis for Seismic Stability of the Soldier Pile Wall Using the Conditional Random Finite-Element Method. Int J Geomech 2022;22(10):04022159. https://doi.org/10.1061/(ASCE)GM.1943-5622.0002534.
[20] Chen XJ, Fu Y, Liu Y. Random finite element analysis on uplift bearing capacity and failure mechanisms of square plate anchors in spatially variable clay. Eng Geol 2022;304:106677.
[21] Cheng P, Guo J, Yao K, Chen X. Numerical investigation on pullout capacity of helical piles under combined loading in spatially random clay. Mar Georesour Geotechnol 2022:1–14.
[22] Cheng P, Liu Y, Li YP, Yi JT. A large deformation finite element analysis of uplift behaviour for helical anchor in spatially variable clay. Comput Geotech 2022;141:104542.
[23] Johari A, Kalantari AR. System reliability analysis of soldier-piled excavation in unsaturated soil by combining random finite element and sequential compounding methods. Bull Eng Geol Environ 2021;80(3):2485–507.
[24] Vanmarcke E. Random fields: analysis and synthesis, 1983. Cambridge: MIT Press; 1983.
[25] Li CC, Der Kiureghian A. Optimal discretization of random fields. J Eng Mech 1993;119(6):1136–54.
[26] Fenton GA, Griffiths D. Bearing-capacity prediction of spatially random c φ soils. Can Geotech 2003;40:54–65.
[27] Rouhani S, Srivastava RM, Desbarats AJ, Cromer MV, Johnson AI. Geostatistics for environmental and geotechnical applications. ASTM International; 1996.
[28] Parsons RL, Frost JD. Evaluating site investigation quality using GIS and geostatistics. J Geotech Geoenviron Eng 2002;128(6):451–61.
[29] Webster R, Oliver MA. Geostatistics for environmental scientists. John Wiley & Sons; 2007.
[30] Matheron G. Principles of geostatistics. Econ Geol 1963;58(8):1246–66. https://doi.org/10.2113/gsecongeo.58.8.1246.
[31] Isaaks EH, Srivastava RM. Applied geostatistics. New York: Oxford University Press; 1989. p. 561.
[32] Cherubini C. Reliability evaluation of shallow foundation bearing capacity on c′ φ′ soils. Can Geotech J 2000;37:264–9.
[33] Cami B, Javankhoshdel S, Phoon KK, Ching J. Scale of fluctuation for spatially varying soils: estimation methods and values. ASCE-ASME Journal of Risk and Uncertainty in Engineering Systems, Part A: Civil Engineering 2020;6(4):03120002.
[34] Phoon KK, Kulhawy FH. Evaluation of geotechnical property variability. Can Geotech J 1999;36:625–39. https://doi.org/10.1139/t99-039.
[35] Rahman MM, Nguyen HBK. Applications of random finite element method in bearing capacity problems. Xpert Publishing Services; 2012.
[36] USACE. Engineering and design: Introduction to probability and reliability methods for use in geotechnical engineering. Engineer Technical Letter. Washington, DC: USACE 1997.
[37] Johari A, Gholampour A. A practical approach for reliability analysis of unsaturated slope by conditional random fnite element method. Comput Geotech 2018;102:79–91. https://doi.org/10.1016/j.compgeo.2018.06.004.
[38] Johari A, Talebi A. Stochastic analysis of rainfall-induced slope instability and steady-state seepage flow using random finite-element method. Int J Geomech 2019;19(8):04019085.
[39] Naderi M.A. Determination of the critical slip surface in slope stability analysis (Doctoral dissertation 2013, Eastern Mediterranean University (EMU)-Doğu Akdeniz Üniversitesi (DAÜ)).
[40] Qi XH, Li DQ. Effect of spatial variability of shear strength parameters on critical slip surfaces of slopes. Eng Geol 2018;239:41–9.